THE STRUCTURE OF DETERMINISTIC MASS, SURFACE AND MULTI-PHASE FRACTALS FROM SMALL-ANGLE SCATTERING DATA*

A. YU. CHERNY[1], E. M. ANITAS[1,2], V. A. OSIPOV[1], A. I. KUKLIN[1,3]

[1]Joint Institute for Nuclear Research, Dubna 141980, Moscow region, Russian Federation
E-mail: cherny@theor.jinr.ru
[2]Horia Hulubei National Institute of Physics and Nuclear Engineering, RO-077125 Bucharest-Magurele, Romania
[3]Laboratory for Advanced Studies of Membrane Proteins, Moscow Institute of Physics and Technology, Dolgoprudniy, Russian Federation

Received November 17, 2014

We present general results on small-angle scattering (SAS) from deterministic (*i.e.*, exactly self-similar) mass, surface and multi-phase fractals. We suggest a method of obtaining additional information from SAS data of deterministic mass fractals, such as the fractal iteration number, the scaling factor, and the number of structural units composing the mass and surface fractal. For a multi-phase system, we show that the qualitative question can be answered from SAS data whether one fractal 'absorbs' another one or they are both immersed in a surrounding homogeneous medium. Surface fractals are shown to be constructed as combinations of mass fractals.

Key words: Small-angle scattering, fractal structures, nano/microclusters.

PACS: 61.05.fg, 61.05.cf, 61.43.-j.

1. INTRODUCTION

Recent progress in materials science offers broad prospects for creating novel meta-materials at nano- and micro-scales, including various fractal structures. A fundamental challenge is to understand the relations between their structural and physical properties.

One of the most important experimental technique for investigating nano/micro structures is small-angle-scattering [1], which gives the coherent differential cross section of an irradiated sample as a function of momentum transfer q. This technique allows us to distinguish between the mass and surface fractals [2–4]. The difference arises in the value of the scattering exponent of the power-law decay of SAS intensity in the fractal region, with $I(q) \propto q^{-\tau}$, where $\tau = D_{\rm m}$ for mass fractals and $\tau = 6 - D_{\rm s}$ for surface fractals. Here $D_{\rm m}$ and $D_{\rm s}$ are the mass and surface fractal dimension, respectively, which lie within $0 < D_{\rm m} < 3$ for mass fractals and within $2 < D_{\rm s} < 3$ for surface fractals.

*Paper presented at the conference "Advanced many-body and statistical methods in mesoscopic systems II", September 1-5, 2014, Brasov, Romania.

It was recently shown [5–7] that apart from the dimension, one can extract some additional information about the structural properties of deterministic mass fractal.

Sometimes SAS intensity curve shows various values of the scattering exponents thus representing successive power-law regimes either of 'convex' or 'concave' type, *e.g.*, in liquid metals [8], soils [9], nanocomposites [10], and soft matter [11]. A two-phase model for explaining of 'concave' scattering intensities was suggested in [12]. For the 'convex' scattering curves, a very general model of multi-phase fractal structures was proposed [13] that generalizes the Stuhrmann contrast variation method. The model allows us to understand whether a fractal 'absorbs' another one or they are both immersed in a surrounding homogeneous medium like solvent.

In this paper, we discuss the recent results for mass, surface and multi-phase fractals with an emphasis on practical applications to experimental SAS data.

2. TWO-PHASE MASS AND SURFACE FRACTALS

The coherent differential scattering cross section per unit volume of the sample (scattering intensity) can be calculated by taking into account the randomness of orientations and spatial positions of the fractals. Therefore, they scatter the incident beam independently which, neglecting multiple scattering, leads to

$$\frac{\mathrm{d}\sigma}{\mathrm{d}\Omega}\frac{1}{V'} \equiv I(q) = n\left\langle |A(\boldsymbol{q})|^2 \right\rangle, \tag{1}$$

where V' is the total volume irradiated by the incident beam, n is the concentration of the fractal objects, $\langle \cdots \rangle$ is the ensemble averaging over all orientations of $\boldsymbol{q}$ and, in the case of polydispersity (*i.e.*, variation of the fractal sizes), over the polydispersity distribution. $A(\boldsymbol{q}) = \int e^{i\boldsymbol{q}\boldsymbol{r}}\rho(\boldsymbol{r})\mathrm{d}^3\boldsymbol{r}$ is the scattering form factor (amplitude) of the fractal and $\rho(\boldsymbol{r})$ is its scattering length density (SLD). In practice it is convenient to write down the intensity in terms of the normalized scattering amplitudes. The normalized amplitude is defined in general as

$$F(\boldsymbol{q}) \equiv \int_V \rho(\boldsymbol{r})e^{-i\boldsymbol{q}\boldsymbol{r}}\mathrm{d}^3\boldsymbol{r} \Big/ \int_V \rho(\boldsymbol{r})\mathrm{d}^3\boldsymbol{r}\,. \tag{2}$$

It follows from the definition that $F(0) = 1$, and for a homogeneous system $A(\boldsymbol{q}) = V\rho F(\boldsymbol{q})$ where V is the volume of the fractal support.

At mth iteration, the mass fractal is composed of cubes of the same size $\beta_{\mathrm{s}}^m l_0$, then the scattering amplitude is $A(\boldsymbol{q}) = V_m\rho F_0(\boldsymbol{q}\beta_{\mathrm{s}}^m l_0)\sum_j e^{-i\boldsymbol{q}\boldsymbol{r}_j}$, where V_m is the volume of the cube, $\boldsymbol{r}_j$ are the center-of-mass positions of the cubes, and F_0 is the form factor of a cube of unit size given by $F_0(\boldsymbol{q}) = \frac{\sin q_x/2}{q_x/2}\frac{\sin q_y/2}{q_y/2}\frac{\sin q_z/2}{q_z/2}$.

For deterministic fractals, the scattering amplitude is known analytically, and

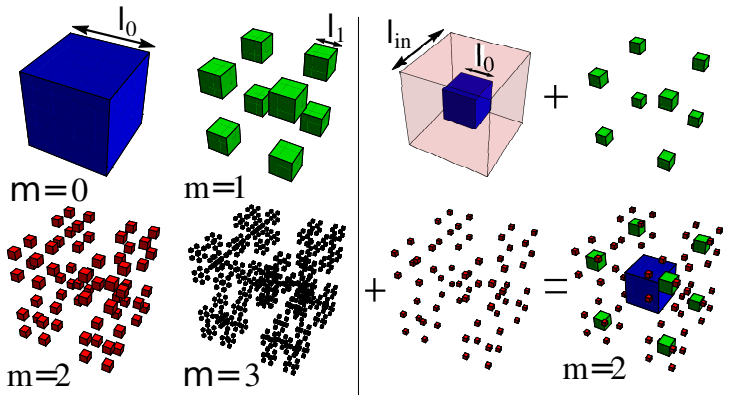

Fig. 1 – (Color on-line) Construction of Cantor fractals in 3D. Left panel: first three iterations of Cantor mass fractals; Right panel: second iteration of 'Cantor-like' surface fractal. At a given iteration, mass fractal consists of cubes with the same size, while surface fractal consists of cubes with different sizes.

for the m-th iteration it can be written as [6, 7]

$$F_m^{\text{mass}}(\boldsymbol{q}) = F_0(\boldsymbol{q}\beta_{\text{s}}^m l_0)G_1(\boldsymbol{q})G_1(\beta_{\text{s}}\boldsymbol{q})\cdots G_1(\beta_{\text{s}}^{m-1}\boldsymbol{q}), \tag{3}$$

where l_0 is the size of the fractal unit at $m = 0$ (see Left panel of Fig. 1), l_1 is the size of the fractal unit at $m = 1$, $\beta_{\text{s}} \equiv l_1/l_0$ is the scaling factor of the fractal, and $G_1(\boldsymbol{q})$ is the generative function, depending on the relative positions of the scattering units inside the fractal. For the Cantor fractal (Fig. 1) it is given by [6] $G_1(\boldsymbol{q}) = \cos(uq_x)\cos(uq_y)\cos(uq_z)$ with $u \equiv l_0(1-\beta_{\text{s}})/2$.

Eq. (3) enables an effective computation scheme, which allows us to obtain analytically the normalized scattering intensity $I_m(q)/I(0) \equiv \left\langle |F_m^{\text{mass}}(\boldsymbol{q})|^2 \right\rangle$, to obtain all the three main regions (Guinier, fractal and Porod, see Fig. 2), and to calculate the radius of gyration of the fractal. In the fractal region the scattering curves fall off as q^{-D} with D being the fractal dimension [2–7]. Fig. 2a shows typical scattering intensities at $m = 3$ for the $3D$ Cantor fractal at different values of β_{s}. As expected, all the three regions are present, each with the corresponding scattering exponents.

Surface fractals can be constructed as sums of mass fractals (Right panel of Fig. 1). Then the normalized scattering amplitude of surface fractals is calculated as a sum of that of mass fractals

$$F_m^{\text{surface}}(\boldsymbol{q}) = \frac{1}{V_{\text{t}}}\left(V_0F_0(l_0q) + \sum_{i=1}^{m} V_i^{\text{mass}}F_m^{\text{mass}}(\boldsymbol{q})\right), \tag{4}$$

where V_{t} is the total volume of the surface fractal and V_i^{mass} is the volume of the mass fractal component at i-th iteration. While calculating F_m^{mass} in Eq. (4), we use G_1 for the Cantor fractal with $u = l_{\text{in}}(1-\beta_{\text{s}})/2$. Fig. 2b shows the scattering

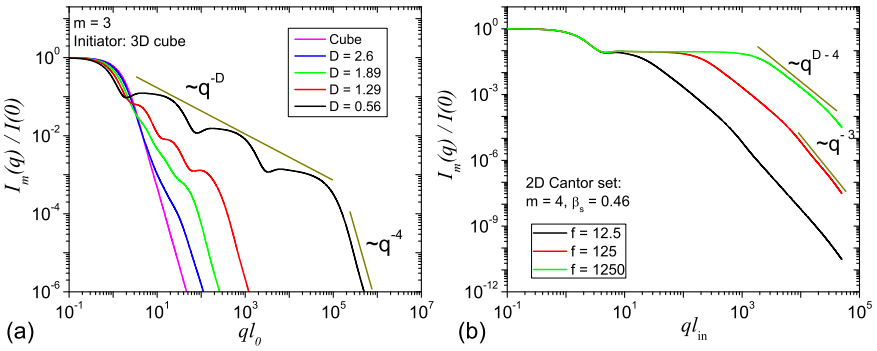

Fig. 2 – (Color on-line) SAS intensities from two-phase polydisperse deterministic fractals with relative variance $\sigma_{\rm r} = 0.4$. a) $3D$ mass fractals. b) $2D$ surface fractals with $D = 1.79$, f is the ratio $l_{\rm in}/l_0$. The condition $f \geqslant 1/(1-2\beta_{\rm s})$ guarantees the absence of overlapping between the structural units of the Cantor surface fractal (see Right panel of Fig. 1).

intensity from a typical $2D$ surface fractal, built as a sum of deterministic fractals. For surface fractals, the intensity in the fractal region decreases as $q^{D_{\rm s}-6}$ in $3D$ (or as $q^{D_{\rm s}-4}$ in $2D$), where $D_{\rm s}$ is the fractal dimension of the fractal surface.

3. MULTI-PHASE MASS/SURFACE FRACTALS

One can construct [13] two different three-phase systems (see Fig. 3a): Type *I* where one phase of size L_2 and SLD ρ_2 is embedded into another phase of size L_1 and SLD ρ_1 and altogether the combined system is further put into a third phase (solvent) of SLD ρ_0, and Type *II* where a mixture of two spatially non-correlated phases put into a third phase. Then the scattering intensity is given by

$$I(q) = a_1/q^{\tau_1} + a_2/q^{\tau_2}, \tag{5}$$

where $a_1 = (\rho_1 - \rho_0)^2 n_1 V_1^2/(L_1/2\pi)^{\tau_1}$, and $a_2 = V_2^2/(L_2/2\pi)^{\tau_2}(\rho_2 - \rho_1)^2 n_1$ for Type *I* and $a_2 = V_2^2/(L_2/2\pi)^{\tau_2}(\rho_2 - \rho_0)^2 n_0$ for Type *II*. By performing a series of measurements at different ρ_0 (the contrast variation method) and fitting each intensity curve with Eq. (5), we obtain the fractal dimensions of each phase, density ρ_1 as the contrast match point in the plot $\sqrt{a_1} \propto |\rho_1 - \rho_0|$, and the value of $n_1 V_1^2/(L_1/2\pi)^{\tau_1}$, see Fig. 3b. Here, n_1 and n_2 are the concentrations of the objects for the two phases.

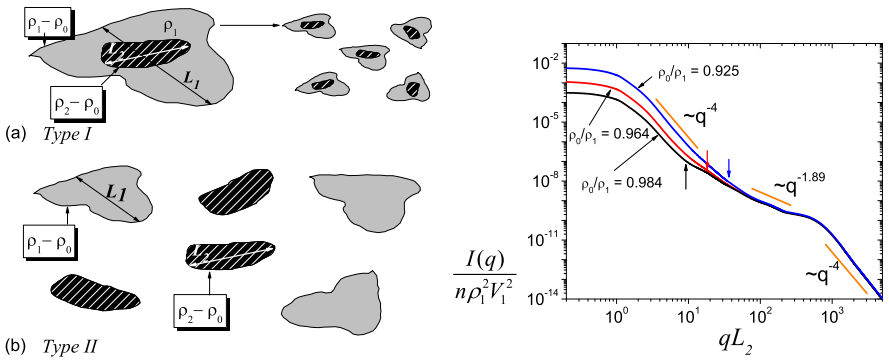

Fig. 3 – (Color on-line) a) Two types of the three-phase systems. b) SAS intensities from multi-phase systems for various values of the solvent ρ_0 (method of contrast variation).

4. CONCLUSIONS

In the papers [5–7], we constructed the 3D deterministic mass fractals, whose dimensions are controlled by the scaling factor of fractal. The SAS intensities from these deterministic fractals were calculated analytically. It was shown [7] that one can extract a number of parameters from the intensity: the fractal dimension from the generalized power-law decay $I(q) \propto q^{-D}$, the scaling factor from the period in the logarithmic scale, the number of fractal iteration from the period of $I(q)q^D$, the lower and upper fractal edges from this diagram as the beginning and end of the 'periodicity region' and the total number of structural units, of which the fractal is composed, from $N_m = (1/\beta_s)^{mD}$.

In Ref. [13] we derived analytical expressions for SAS intensity from a mixture of correlated (Type *I*) and, respectively, uncorrelated (Type *II*) multi-phase systems, characterized by the presence of power-law regimes with various scattering exponents. The interpolating formula (5) can be used to fit experimental SAS data from mixtures of multi-phase systems which show a variation of the crossover position with SLD of any of the containing phase. The implementation of the contrast variation method to the coefficients a_1 and a_2 in Eq. (5) enables us to distinguish between Type *I* and Type *II* structures.

REFERENCES

1. O. Glatter, O. Kratky, *Small-angle X-ray Scattering* (London, & Academic Press, 1982).
2. P. W. Schmidt, X. Dacai, Phys. Rev. A **33**, 560 (1986).
3. J. E. Martin, A. J. Hurd, J. Appl. Cryst. **20**, 61 (1987).
4. P. W. Schmidt, J. Appl. Cryst. **24**, 414 (1991).
5. A. Yu. Cherny, E. M. Anitas, A. I. Kuklin, M. Balasoiu, V. A. Osipov, J. Surf. Invest. **4**, 903 (2010).
6. A. Yu. Cherny, E. M. Anitas, A. I. Kuklin, M. Balasoiu, V. A. Osipov, J. Appl. Cryst. **43**, 790 (2010).
7. A. Yu. Cherny, E. M. Anitas, V. A. Osipov, A. I. Kuklin, Phys. Rev. E **84**, 036203 (2011).
8. Yu. S. Kovalev *et al.*, J. Non-cryst. Solids **353**, 3532 (2007).
9. G. N. Fedotov *et al.*, Dokl. Chem. **412**, 55 (2007).
10. M. E. Dokukin *et al.*, B. Russ. Acad. Sci. Ph. **71**, 1602 (2007).
11. V. V. Isaev-Ivanov *et al.*, Phys. Solid State **52** 1063 (2010).
12. E. M. Anitas, Eur. Phys. J. B **87**, 139 (2014).
13. A. Yu. Cherny, E. M. Anitas, V. A. Osipov, A. I. Kuklin, J. Appl. Cryst. **47**, 198 (2014).